Investigations on Self-extinction of Incense Sticks

A. Ve. Sowriraajan [ID]*, A. Shivakumar, Sachin Payyanad, C. S. Bhaskar Dixit and H. S. Mukunda, FCRC, Jain (Deemed-to-be-University), Bangalore, Karnataka, India

Abstract. A low-probability but serious self-extinction of smouldering incense sticks is an undesirable characteristic. This paper reports the investigations on its cause and remedy, conducted for an incense stick manufacturer. Measurement of smouldering rate and surface temperature of glowing incense stick tip of several known compositions were made by recording the time required for the propagation of smoldering front and using thermal camera respectively. Several possible explanations like presence of (a) phosphorous, potassium, and sodium related compounds, (b) inadvertent inclusion of inorganic compounds, and others ruled out the role of phosphorous and related compounds, and a simple role of inorganic compounds despite the fact that defective incense sticks invariably contained large fraction of silica (SiO_2) as revealed by scanning electron microscopy/ energy dispersive X-ray diffraction (SEM/EDX). Ultimately the issue was traced to the presence of antigorite that must have got infused into the incense sticks through termite mud into the raw materials. X-ray diffraction (XRD) of incense stick samples confirmed silica is in the form of α-quartz associated with antigorite in all defective samples and also in termite mud infested sample. Thermal studies of the incense sticks using differential thermal analysis (DTA) show endothermic decomposition of defective samples at 550 to 580°C and is also confirmed through differential scanning calorimetry (DSC) which shows an endothermic peak around 576°C corresponding to the endothermic phase transformation temperature of antigorite. It is therefore inferred that the presence of materials like antigorite in combination with α-quartz in incense sticks produce significant endothermal decomposition leading to self-extinction. The primary practical cause has been traced to termite mud infusion into the raw materials used for making the incense sticks.

List of Symbols

CG	Normal sample
CB	Extinguishing sample
C1–C9	Samples of different compositions
C3	Termite mud infested sample
D	Diameter of the sample (mm)

*Correspondence should be addressed to: A. Ve. Sowriraajan, E-mail: ave.sowriraajan@ jainuniversity.ac.in

Published online: 10 March 2023

Ext	Extinguishing
G1–G3	Samples with guar gum as binder
L	Length of the sample (cm)
Mo	Initial mass (g)
M1–M6	Market samples
S/T	Sand/Termite mud
f_w	Moisture percentage
ρ	Density (kg/m^3)
$\dot{r}$	Smoldering rate (mm/min)
T_s	Surface temperature (°C)
ε	Emissivity

1. Introduction

The incense stick industry is prevalent in religiously dominated eastern countries. The major composition of incense sticks is similar from different manufacturers and brands. Typically, incense stick comprises of finely ground powder of wood, charcoal, and adhesives (locally termed as *Jigit*). The constituents are thoroughly mixed by adding water and this mixture is then extruded to form a coating on bamboo stick with a thickness of about 1 mm [1, 2]. It is then impregnated with fragrance. Current work addresses the much-disliked low-probability self-extinction problem of smouldering incense sticks. A manufacturer provided us with the composition along with *CG* (steady smouldering) and *CB* (self-extinction after ignition and initial burn) samples. The manufacturer also indicated that the rejection was to the extent of 0.1 to 0.2%. While this did not appear significant, it was unacceptable as the incense sticks lit on religious occasions are expected to burn completely and self-extinction is deemed highly inauspicious. It is in this backdrop the current investigations are undertaken. A survey of literature [1–10] indicated that the studies are either on material characterisation, understanding the smouldering process, product development or fine tuning/economizing composition, and their ill effects on air pollution. For example, Yadav et al. [1, 2] worked on characterisation of Indian Incense sticks reporting physical, chemical, and mineralogical characteristics. The XRD results of raw incense indicates the presence of carbon, silica, calcite, and iron oxide at a higher amount. But the influence of these materials in the smouldering characteristics is not reported. Studies by Mukunda et al. [3], Lin et al. [4], and Yamazaki et al. [5] are concerned with the experimental and modelling studies on the smouldering phenomena of incense sticks under various environmental conditions and the smouldering rate measured by them in the atmospheric pressure is in the range of 3.1 to 4.6 mm/min.

Cheng et al. and others [6–10] have worked on incense smoke characterisation and dynamics in indoor environment and estimated the incense aerosol generation rate as a function of time and the aerosol removal rate constant. The study [6] focuses on how the particulates generated deposit inside respiratory tract leading to breathing problems. Yang et al. [8] has burnt the different market samples and obtain an average burn rate of 4.1 mm/min.

It is observed that the problem of self-extinction of incense stick smouldering has never been addressed although there are some studies on blow-off of incense

sticks with different orientation and air flow in confined compartments. The present work is related to the investigations on self-extinction of the incense sticks aimed at uncovering the reasons for it.

2. Experimental Studies

Experimental studies were conducted on incense stick samples and the parameters studied include moisture percentage (f_w), density (ρ), ash percentage, smouldering rate ($\dot{r}$), and surface temperature (T_s). In order to understand the spectrum of issues, samples of the ingredients and several batches of incense sticks were obtained from the concerned manufacturer. Additional samples from popular brands were also included into the investigation.

Moisture percentage (f_w) is determined by traditional air oven method in which the samples are subjected to a temperature of $105 \pm 2°C$ up to 4 h till the change in mass obtained after desiccating the sample and verified using a digital electronic balance of 1 mg accuracy reaches a stable value. Density (ρ), discussed here is the bulk density obtained from the ratio of mass (m) to the dimensional volume (V) of each sample. Ash percentage is the percentage mass fraction of the material left after subjecting the sample to a temperature of $650 \pm 20°C$ in a muffle furnace. The studies were conducted inside the lab with quiescent atmospheric conditions at temperature of 27°C, with negligible ambient air velocity.

Incense sticks were mounted on a vertical stand having holes arranged on its flat surface of 6.5 cm × 6.5 cm in a 10 × 10 (nos.) square matrix. They were ignited using safety matches. Videos of experiments were captured using Nikon D5300, DSLR camera. Simultaneously, the surface temperature is measured using a thermal camera (make FLIR-T62101) by positioning the camera horizontally at a distance of 1 m from the sample. There were settings required on the focus of the beam capturing the thin high temperature zone. The initially chosen settings were 2000°C and 200°C. Finally, they were adjusted to the peak value obtained instead of a maximum of 2000°C. Emissivity (ε) of the camera is set to 0.9. The smouldering rate of the sticks was obtained by recording time required for the downward propagation of the reaction front.

Other investigative equipment used include Fourier Transform Infrared Spectroscopy (FTIR, make: Thermospectronic Nicolet iS50), Scanning Electron Microscopy and Energy Dispersive X-ray diffraction (SEM/EDX, make: JEOL, JSM-IT300, Japan), Thermogravimetry DT/TGA (Shimadzu DTG-60) and X-ray diffraction (XRD, make: Rigaku Ultima IV), in a progressive approach towards unravelling the issue.

FTIR was operated in the Attenuated Total Reflection (ATR) mode and the results are obtained as % absorbance vs wave number (cm^{-1}). The equipment uses diamond crystal, KBR beam splitter and DTGS detector. Scan rate set for 32 scans for back ground and sampling. X-ray diffraction analysis was carried out using Rigaku Ultima IV diffractometer for powder, under the following technical conditions: angled recording area 2θ from 5 to 85° and/or 90°, scan speed 5 deg/min, step width 0.02°.

DT/TGA analysis of the samples were carried out using Shimadzu DTG-60 at 20–1000°C temperature range, with a heating rate of 10°C/min in an atmosphere of air. DSC analysis were carried out using Shimadzu DSC-60 at 10°C/min heating rate for temperature range of 30°C to 600°C under Nitrogen. SEM/EDX analysis were carried out by spreading powder on double-sided carbon tape followed by 10 min of gold sputtering. The SEM images were captured at various magnifications and analysis with 20 μm area magnification is presented. The micro elemental analysis was carried out using EDX by selecting 10 different spots and averaging the results obtained. The efforts to unravel the cause along with insights obtained during the investigations are outlined in the following sections.

3. Results and Discussions

3.1. Smoulder Tests

All the data on the studies of the samples are listed in Table 1. The various terms used are also explained in the Table. Several experiments were done by igniting the samples to get a comparison of various parameters influencing the smouldering rate of the candidate problem sample (CB in Table 1) with that of samples bought from the market. The reported values are the average of minimum of three samples. These generally showed that most of them were smouldering at rates of 2.5 to 3.6 mm/min. The data on the first two samples from the industry shows that the first one (CG) smoulders well, but the second one (CB) extinguishes after some time. The samples with the addition of guar gum (samples G-1 to G-3) and sand (C1 and C2) show a decreased smouldering rate compared to all other samples and the sample C3 which is infested with the termite mud extinguishes after some time similar to sample CB.

Figure 1 shows the temperature data captured using thermal imaging camera for CG, CB, and C3 samples and it can be seen that the smouldering surface temperature of CG samples is about 630°C and in the case of CB and C3 samples the temperature continuously drops from 630°C and by the time stick extinguishes which was physically observed, the measured surface temperature was about 490°C. The time scale over which the decrease from ∼ 630 to 490°C occurs is 100 s for CB and 50 s for C3 sample. This time scale depends on the rate of reduction in surface temperature of the samples CB and C3 (with different percentages of antigorite and α-quartz (as inferred from work discussed later in Sect. 3.3) that occurs due to absorption of heat by the decomposing antigorite and α-quartz. The temperature fall rate of 1.5 to 3 K/s is dependent on this feature. It should also be noted that there will be heat losses from the surface through radiation into the surroundings and conduction into the solid over a time. Below a temperature of 490°C, the surface heat release is not adequate to maintain the thermal balance, the emission of volatiles and smoke ceases and the smouldering process stops. These are specifically set out in Fig. 2 that carries still photographs sliced from a video of the smouldering stick, CB at several intervals. It is clear that the stick has stopped smouldering at 100 s and the temperature at that moment was 490°C.

Table 1
Results on the Incense Sticks

Sample	Composition					Dimensions		Parameters					
	Wood %	Charcoal %	Jigit %	Guar %	S/T %	L cm	D mm	f_w %	m_o g	ρ kg/m³	Ash %	$\dot{r}$ mm/min	Mean T_s °C
CG	40	45	15	0	0	20.5	3.08	8.25	1.63	1067	15.1	3.6	640
CB	40	45	15	0	0	18.7	3.26	8.19	1.38	880	20.0	Ext	490*
M-1	NA	NA	NA	NA	NA	17.8	3.16	8.21	1.39	998	7.9	2.6	630
M-2	NA	NA	NA	NA	NA	22.8	3.12	8.22	1.94	1111	14.7	3.5	610
M-3	NA	NA	NA	NA	NA	20.1	3.08	8.16	1.67	1112	14.1	2.5	640
M-4	NA	NA	NA	NA	NA	18	2.82	8.11	1.01	899	6.9	2.9	615
M-5	NA	NA	NA	NA	NA	18	2.96	8.23	1.01	813	20.9	3.3	620
M-6	NA	NA	NA	NA	NA	17.5	3.18	8.14	1.22	876	14.8	2.9	630
G-1	33	50	8	9	0	4.14	8.63	3.24	1.62	668	18.8	2.2	610
G-2	33	50	8	9	0	4.11	8.56	8.21	1.79	755	17.1	1.6	560
G-3	33	50	8	9	0	4.14	8.46	15.1	1.72	740	17.7	1.5	600
C1	33	37.5	12.5	0	17S	3.72	8.73	5.26	1.69	760	35	1.91	630
C2	27.5	31	10.5	0	31S	3.78	8.76	5.55	1.92	844	41.5	1.83	600
C3	28.5	32	10.7	0	29T	3.37	8.5	5.32	1.53	800	38.1	Ext	490*
C4	85	0	15	0	0	3.93	8.78	5.22	1.29	542	12.5	2.3	620
C5	0	85	15	0	0	3.67	8.85	6.42	1.74	770	23	2.2	610
C6	40	45	15	0	0	3.97	8.79	5.46	1.59	662	20	2.5	640
C7	45	40	15	0	0	3.51	8.71	6.22	1.37	657	19	2.2	640
C8	65	20	15	0	0	3.82	8.74	6.34	1.35	591	14	1.9	605
C9	20	65	15	0	0	3.63	8.71	7.11	1.53	706	23	2.6	635

M-1 to M-6 Market samples, *CG* Normal sample from reference industry, *CB* Extinguishing sample from reference industry, *G-1, 2, 3* Guar gum related samples made in the laboratory; *C1 to C9* Samples specially made with different compositions to determine the effect of sand/termite mud and charcoal, *S/T* Sand or termite infested wood powder, *Ext* extinguishing, *T_s at extinction
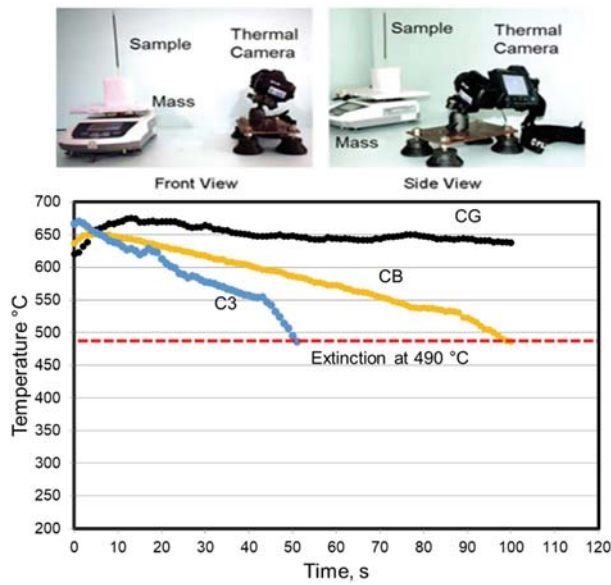
Figure 1. *Top*: **Front and Side view of experimental arrangement;** *Bottom*: **Smoldering surface temperature vs time plot for CG, CB, and C3 incense stick samples.**

Figure 2. Instantaneous smoldering pictures of CB sample including extinction.

Table 2 presents the data of mean smouldering rates of CG and CB samples from the manufacturer having incense lengths of 175 to 180 mm. Results indicate CG incense sticks smoulders completely with a mean smouldering rate of 2.9 to 3.6 mm/min while the CB samples smoulder for less than 130 s and then extinguish.

Table 2
Smouldering Studies of Normal (CG) and Extinguishing (CB) Samples with 8% Moisture

Sample	Smouldering length (mm)	Period of smouldering (min)	Smouldering rate (mean) mm/min	Remarks
CG	175	48.6	3.6	Smoulders completely
CG	176	53.3	3.3	Smoulders completely
CG	180	62.3	2.9	Smoulders completely
CB	5.0	2.1	Ext	Extinguishes in 128 s
CB	4.5	2.0	Ext	Extinguishes in 120 s
CB	4.5	2.1	Ext	Extinguishes in 124 s

3.2. Possible Explanations

Examination of literature to explore the reasons for extinction provided no clear direction excepting possibilities that would need to be studied. These were the three possibilities: (a) presence of significant amount of inorganics like compounds of phosphorous or potassium ingredients in the wood powder, due to the basic biomass drawn from trees growing in a fertilizer dominant soil. This is because some of the phosphorous compounds like phosphates has been known to be a combustion inhibitors with action in the condensed phase and potassium compound forming a low temperature melt layer of the oxides covering the active surface, (b) inadvertent presence of significant amount of inorganic material (sand and mud related) due to poor handling that could have led to very reduced amount of active ingredients and (c) the possibility of guar as a compound having entered into the incense sticks leading to lower burn rates and possible extinction. Each of these was to be examined to uncover the possible reason for extinction.

In the case (a) related to phosphorous compounds, Lowden and Hull [11] state that "phosphorus-based compounds are some of the best-known fire-retardant treatments for timber. They are considered to work mainly in the condensed-phase, by promoting char formation and depriving the gas-phase of further volatile decomposition products". The method of working is described in which in the condensed-phase, the thermal decomposition of inorganic phosphorus-based compounds forms phosphoric acid, which converts to pyrophosphate and water. The water released dilutes the oxidising gas-phase and both phosphoric acid and pyrophosphate promote the dehydration of terminal alcohols from wood, cross linking the cellulose structure, promoting wood's natural ability to char. While the retarding property was thus a well-established feature, whether the quantum of phosphorous transport into biomass grown in fertilized lands was large enough to resist propagation of smouldering combustion front was unclear. Further, the work of Ovington and Madgwick [12] showed that the contents of potassium, sodium, and phosphorous are between 0.03 to 0.1% in the biomass and so, the naturally ingrained compounds would most likely not be responsible for the

observed self-extinction. In order to strengthen this inference, particularly with regard to phosphorous, FTIR and SEM/EDX studies were conducted.
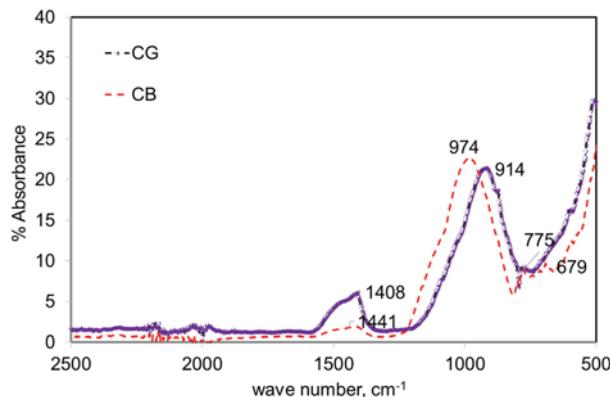
Figure 3 shows the FTIR absorbance spectra. These indicate the presence of phosphorus groups like $-PCH_2$ and $PO3^-$ [$-PCH_2$:1408 cm^{-1} (CG), 1441 cm^{-1} (CB); $-PO3^-$: 914 cm^{-1} (CG), 974 cm^{-1} (CB)] and both samples of CG and CB have similar peaks and it is clear that phosphorous related compounds make no difference to the smouldering behaviour.

In order to consider the second possibility (b) of the inadvertent presence of significant amount of inorganic material, several sticks of commercial nature were procured and tested (M1 to M6). Of these, sample M5 has an ash fraction of 20.9% which is same as the ash fraction of sample CB, but it smoulders at a rate of 3.3 mm/min with a mean surface temperature of 620°C (see Table 1). This implied that one would need to look for causes beyond the ash fraction, per se. The suggestion that the production of select groups of incense sticks carrying guar gum as adhesive had problems of self-extinction [13] was explored. In the case of explanation (c), the samples prepared with guar gum (G1 to G3 in Table 1) showed low smouldering rates, but always had a steady rate. While, why the smouldering rates got lowered itself would be a separate question, the fact that even at reasonable percentages ($\sim$ 9%) there was steady smoulder implied that guar gum could not be linked to any possible extinction.

3.3. Further Considerations

In order to examine whether the extinguishing samples had any other compound that could cause the problem, the samples were subject to SEM/EDX study. Figure 4 shows the SEM images of CG and CB samples in which 10 spots were chosen and averaged for EDX analysis.

The results are set out in Tables 3 and 4 for both the classes of samples. Using these data probable combinations of oxidized compounds that could be present naturally in wood is arrived as shown in Table 5.

Figure 3.   Absorbance FTIR spectra of incense sticks.

Figure 4.   SEM images of CG (*Left*) and CB (*Right*) samples with EDX spots.

One can observe from Table 5 that the CB incense stick samples have higher probable percentage of inorganics (58%) which has retarding potential compared to sample CG (32.3%) and one can notice that the sample CB has a very large fraction of silica compared to CG samples. Since most compounds by themselves are stable in the temperature range (up to about 700°C), it is inferred that silicon in all likelihood as complex silicates as well as SiO_2 could be suspected as a candidate for the observed extinction. This was also because there is a possibility of sand or mud getting mixed with biomass when being pulverized in a not-so-clean environment.

To uncover the effect of sand on smoldering that would have entered into biomass powder during the process of pulverization, two samples were made by adding a significant amount of finely powdered and sieved sand into the composition.

Table 3
Elemental Composition as Indicated by SEM/EDX Analysis of CG Sample

Element	Spot 1	Spot 2	Spot 3	Spot 4	Spot 5	Spot 6	Spot 7	Spot 8	Spot 9	Spot 10	Avg
B	4.3	5.6	0.4	5.7	0.3	0.2	5.5	5.3	5.9	5.4	3.9
C	61.7	63.6	87.7	74.7	40.2	58.4	65.3	88.3	76.9	71.5	68.8
N	0.0	0.0	2.3	0.0	0.0	0.1	0.0	0.0	0.0	0.0	0.3
O	21.1	23.2	7.9	14.0	40.5	21.2	23.7	5.0	11.9	14.6	18.3
Mg	1.4	1.2	0.1	0.3	0.9	0.4	0.2	0.0	0.6	0.4	0.5
Al	0.5	0.3	0.1	0.2	0.6	0.9	0.2	0.0	0.3	0.5	0.4
Si	0.9	0.4	0.1	0.6	0.9	1.6	0.5	0.0	0.4	0.6	0.6
P	2.9	1.5	0.3	1.8	2.4	5.6	1.8	0.9	1.4	1.9	2.0
Cl	0.4	0.2	0.3	0.3	0.2	0.6	0.1	0.0	0.3	0.5	0.3
K	2.9	2.0	0.1	0.5	0.6	2.6	1.4	0.3	0.8	0.5	1.2
Ca	3.8	2.2	0.7	1.9	13.6	8.5	1.1	0.1	1.6	4.0	3.7
	100.0	100.0	100.0	100.0	100.0	100.0	100.0	100.0	100.0	100.0	100.0

Table 4
Elemental Composition as Indicated by SEM/EDX Analysis of CB Sample

Element	Spot 1	Spot 2	Spot 3	Spot 4	Spot 5	Spot 6	Spot 7	Spot 8	Spot 9	Spot 10	Avg
B	0.1	4.9	8.0	5.4	5.6	5.2	5.2	0.1	0.1	0.8	3.5
C	4.6	39.3	78.0	71.5	43.5	54.0	55.9	4.2	24.1	47.5	42.3
N	0.6	2.6	0.0	0.0	4.3	0.2	2.0	0.3	0.0	0.0	1.0
O	47.0	36.6	9.9	21.1	34.7	19.9	21.3	46.9	31.8	28.1	29.7
Mg	0.3	1.1	0.0	0.0	0.9	0.1	0.1	0.2	0.2	0.0	0.3
Al	0.6	2.5	0.1	0.0	1.4	0.4	0.6	0.4	2.2	0.1	0.8
Si	45.9	8.0	2.1	0.3	6.7	19.3	14.0	47.3	34.8	21.7	20.0
P	0.6	1.0	0.8	1.0	0.9	0.5	0.5	0.5	1.7	1.2	0.9
Cl	0.1	0.2	0.0	0.0	0.1	0.1	0.0	0.1	0.3	0.0	0.1
K	0.2	1.6	0.1	0.5	0.8	0.1	0.2	0.0	1.3	0.5	0.5
Ca	0.1	2.2	0.9	0.3	1.3	0.2	0.4	0.1	3.5	0.1	0.9
	100.0	100.0	100.0	100.0	100.0	100.0	100.0	100.0	100.0	100.0	100.0

Table 5
The Probable Inorganic Material Composition Obtained from Elemental Composition Data

Probable compounds	CG	CB	Retarding potential
B_2O_3	12.4	11.4	Yes
C	67.7	42.0	No
KCl	0.6	0.2	Yes
MgO	0.9	0.5	Yes
Al_2O_3	1.0	2.3	Yes
SiO_2	1.3	34.2	Yes
P_2O_5	4.7	2.0	Yes
$CaCO_3$	9.4	2.3	Yes
Others*	2.0	5.1	–
	100.0	100.0	

*Nitrogen compounds are considered here.

These are set out in Table 1 as C1 and C2. The ash content was taken to as high a value as 41.5%. Interestingly the sticks smoulder at lower rates of $\sim$ 1.8 mm/min with surface temperature in the range of 600°C +. The reason for reduction in the smoldering rate of C1 and C2 samples can be attributed to the abrupt changes to quartz at 575°C, where α-quartz transforms to β-quartz as observed from the work of Raman and Nedungadi [14] as also supported by the observations of Weber and Greer [15] which indicate that the α to β transition of quartz occurs at a temperature of 571 to 573°C. However, since this transition enables depression in smouldering rate, but not extinction (of sample CB) a combination

of silica and silicates entering the product through sources like clay/termite mud was further considered.

Momah and Okeiman [16] indicated the presence of serpentinites like antigorite, $Mg_3Si_2O_5(OH)_4$ in the termite mound soil that are rich in hydroxyl groups in their complex structure and these may break down at high temperature. Hrsak et al. [17], Zulumyan et al. [18], and Ferrand [19] showed that the antigorite decomposes at a temperature of 600 to 800°C and it occurs in steps—first, a slow de-hydroxylation process that breaks low-energy OH bonds and then, high-energy OH bonds are broken. Also, the work of Perrillat et al. [20] shows that upon heating the antigorite will lead to talc like phase and it is known that talc is used as fire retardant material.

Now, to uncover the if there is a possible termite infestation of the sample CB, a sample C3 was prepared by using the raw materials and the termite mud that was sourced from termite-ridden wood within the laboratory and smouldered. The behaviour of the sample was similar to sample CB and it did not smoulder beyond 50 s and there was a continuous reduction in the surface temperature as shown in the Fig. 1 and the surface temperature at the time of extinction was 490°C. The reasons for the difference in the observed extinction time scales of both samples CB and C3 has been discussed in detail in the Sect. 3.5. To determine the reasons for the extinction of the sample C3 which contains antigorite in the form of termite mud, a detailed thermal analysis with the aid of DT/TGA and DSC were performed. The details of thermal analysis are discussed below.

3.4. Differential Thermal Analysis DT/TGA & DSC Studies

The results of thermal analysis are set out in Fig. 5 on samples of CG, CB, C3 and C2. DT/TGA analysis was conducted in an atmosphere of air. The exothermicity at 330 and 410°C is due to the volatile reaction with air at these temperatures with the former coming from aromatic component of the incense stick and the latter due to the volatiles of biomass. One can see the behaviour of CB and C3 samples is identical in both the cases. Also, one can observe from the TGA that the mass retention of the samples C3 and CB is up to a level of $\sim 35\%$, while the CG sample burns to around 5% of its mass at a temperature of 550–580°C essentially due to differences in the ash fraction.

The results of DSC analysis of the samples are set out in Fig. 5b. While the samples C2, C3 and CB show an endothermic peak at a temperature of 570 to 576°C, sample CG shows no endothermicity in this temperature range. It is clear that the samples show up the presence of common endothermicity inducing components in C2, C3, and CB. Sample C2 was specifically produced by adding sand into a composition that is otherwise identical to CG. Sand constituted of α-quartz whose transformation to β-quartz with associated endothermicity is the obvious reason for the reduction of the smoldering rate in the case of C2. The near identical behaviour of endothermicity in terms of temperature indicates that α-quartz is involved in the process. To uncover the constituents in the samples C3 and CB, XRD studies were performed next.
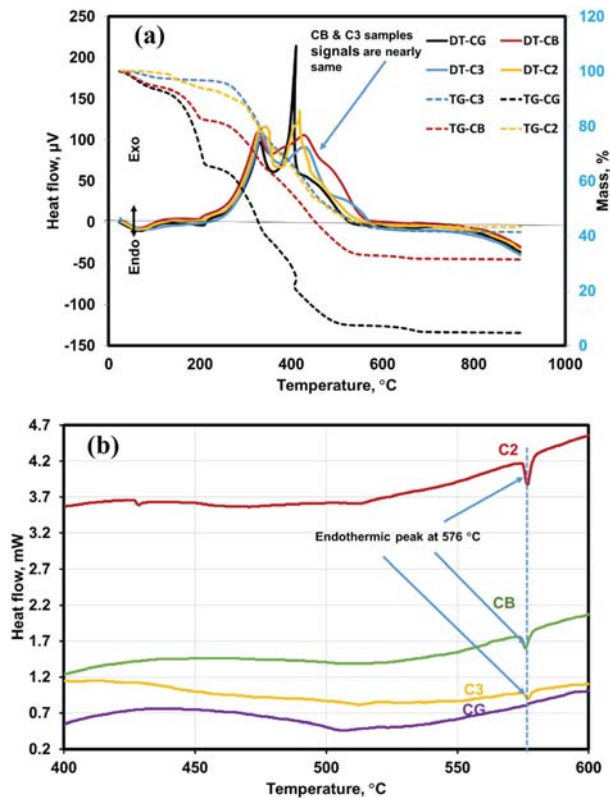
Figure 5. (a) DT/TGA curves of C2, C3, CG, CB samples in air; (b) DSC analysis of C2, C3, CG, CB samples (in nitrogen).

3.5. X-Ray Diffraction (XRD) Studies

In order to obtain the mineralogical compositions of the samples C2, C3, CB, and CG, XRD studies were performed and the results are compared as shown in Fig. 6, and quantified in Table 6 using Match! Software version 3.3. These results indicate strong presence of silica in the form of α-quartz in the samples C2, C3, and CB and also shows the presence of antigorite in C3 and CB samples, whereas the results of sample CG indicate the presence of only calcite as a major compound. If we obtain the percentage of antigorite in the inorganics of C3 and CB samples, we get 15.4% and 8.1% respectively. Also it can be seen that the sample C3 has higher percentage of α-quartz compared to sample CB. These higher percentage of inorganics in the sample C3 cause it to extinguish faster compared to sample CB as indicated in the Sect. 3.1. From these XRD studies, the presence of antigorite and α-quartz in the sample CB and C3 were traced and it is inferred that their thermal decomposition is responsible for extinction of the samples. The analysis was further extended by performing the XRD for the ash of samples CG, CB, and C3.
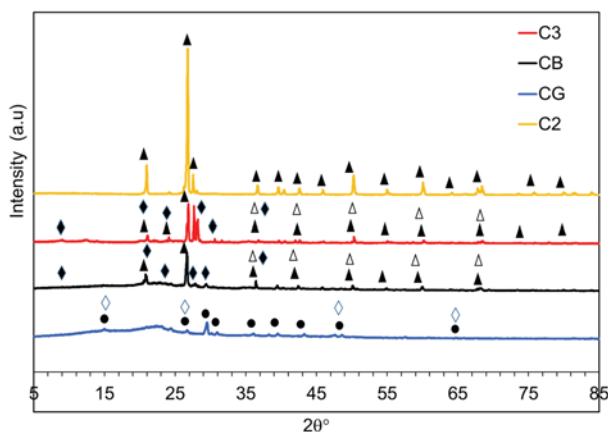
Figure 6. XRD patterns of C2, CG, CB, and C3 samples; Markers: Black triangle—Quartz (SiO_2), Black Diamond—Antigorite; Hollow triangle—Montmorillonite; Black circle—Aragonite ($CaCO_3$); Hollow Diamond—Diopside.

Table 6
Calculated Mineralogical Composition from XRD, All in %

Composition	C2	C3	CB	CG
Silica (quartz), SiO_2	73.3	59.5	53.0	–
Antigorite, $[Mg_3Si_2O_5(OH)_4]$	–	40.5	40.7	–
Montmorillonite, $[Al_{0.86} Fe_{0.1} H Li_{0.08} Mg_{0.14} O_{10}Si_{3.9}]$	–	–	6.3	–
Aragonite, $CaCO_3$	26.7	–	–	61.6
Diopside, $[CaMgSi_2O_6]$	–	–	–	38.4

The ash of the samples CG, CB, and C3 was obtained by placing a known quantity of raw samples in the muffle furnace at 650°C for over 2 h. The obtained ash samples were subjected to XRD and the results were quantified using Match! Version 3.3 software [21], to get the mineralogical composition as shown in Fig. 7. It is observed that the ash of CG sample contains 89.2% of $CaCO_3$ and 10.8% of quartz, while the ash of samples CB and C3 found to have 100% quartz. Further, tests on the ash by adding hydrochloric acid gave effervescence due to release of carbon dioxide indicating the presence of carbonates in the CG sample while this was not observed with CB and C3 samples. Thus, it is concluded that the presence of antigorite with α-quartz alone was responsible for the extinguishment observed in the CB samples.
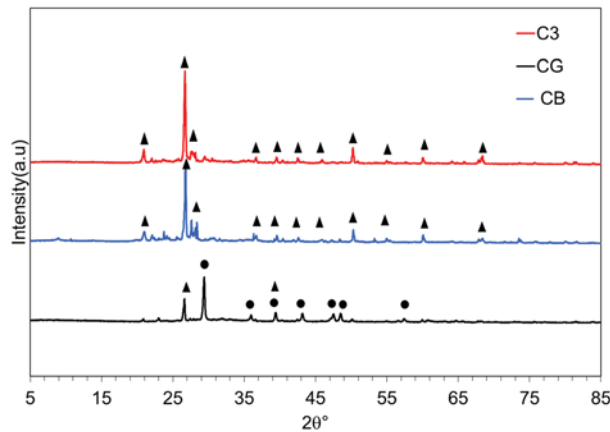
Figure 7. XRD patterns for the ash of CG, CB, and C3 samples; Markers: Black triangle—Quartz (SiO_2), Black circle—Calcite ($CaCO_3$).

3.6. The Extinction Process

Since it is clear that antigorite is present in the extinction samples to a significant extent, the most plausible extinction process must arise from the decomposition of antigorite. Amongst others, references [22–24] have outlined the process of decomposition of antigorite. A simple version involves the decomposition process with the breaking of (Mg–O–Si) and (Si–O–Si) bonds with an overall endothermic reaction, $Mg_3 Si_2O_5 (OH)_4 \rightarrow Mg_3Si_2O_7 + 2H_2O$. Two parts of the extinction processes are dehydroxylation and α to β quartz transformation. These occur in the same temperature range of 550 to 580°C and the decomposition involves release of water. The presence of moisture (with a larger specific heat compared to other gases) just at the surface causes energy absorption from the exothermic reaction. While the quantitative elucidation will await further work, the presence of a significant amount of antigorite as an endothermic agent along with silica as α-quartz seems a highly plausible combination causing extinction.

4. Concluding Remarks

This work was undertaken to seek a possible cause for the observed extinction of some incense sticks and to examine if there is a simple and clear cause for it. Normal (CG) incense sticks smoulder at 2.5 to 3.5 mm/min with surface temperatures between 630 to 650°C while extinguishing (CB) incense sticks self-extinguish at a very early stage. The causes due to the presence of several inorganic ingredients were ruled out and the use of sand allowed the incense stick to smoulder albeit at small rates $\sim$ 1.8 mm/min, even at 41% ash fraction. Finally, the extinction phenomenon in the sample CB is traced to the presence of antigorite and α-quartz in termite mud which upon heating transform to talc like phase and β-quartz respectively along with the release of moisture absorbing energy released in the surface

reaction. While the details of the process await further study, the recommendation to avoid termite infested mud in the ingredients is the practical outcome of this study.

Acknowledgements

Declarations

Conflict of interest The authors have no conflicts of interest to declare. All co-authors have seen and agree with the contents of the manuscript and there is no financial interest to report. We certify that the submission is original work and is not under review at any other publication.

References

1. Virendra Kumar Y, Nisha C, Samreen HK, Areeba K, Raman KR, Kumar P, Shreya M, Gnanamoorthy G (2020) Incense and incense sticks: types, components, origin and their religious beliefs and importance among different religions. J Biol Innov 9:1420–1439. https://doi.org/10.46344/JBINO.2020.v09i06.28
2. Virendra Kumar Y, Bijendra S, Nisha C (2020) Characterization of Indian incense stick powders for their physical, chemical and mineralogical properties. WJEB 9:39–43
3. Mukunda HS, Basani J, Shravan HM, Binoy P (2007) Smouldering combustion of "incense" sticks: experiments and modelling. Combust Sci Technol 179:1113–1129. https://doi.org/10.1080/00102200600970019
4. Lin S, Chow TH, Huang X (2021) Smoldering propagation and blow-off on consolidated fuel under external airflow. Combust Flame 234:111–685
5. Yamazaki T, Matsuoka T, Nakamura Y (2019) Near-extinction behaviour of smoldering combustion under highly vacuumed environment. Proc Combust Inst 37:4083–4090
6. Cheng YS, Bechtold WE, Yu CC, Hung IF (1995) Incense smoke: characterization and dynamics in indoor environments. Aerosol Sci Technol 23:271–281. https://doi.org/10.1080/02786829508965312
7. Yang TT, Lin TS, Chang M (2007) Characteristics of emissions of volatile organic compounds from smoldering incense. Bull Environ Contam Toxicol 78:308–313
8. Yang CR, Lin TC, Chang FH (2006) Correlation between calcium carbonate content and emission characteristics of incense. J Air Waste Manag Assoc 56:1726–1732. https://doi.org/10.1080/10473289.2006.10464577

9. Lin TC, Krishnaswamy G, Chi DS (2008) Incense smoke: clinical, structural and molecular effects on airway disease. Clin Mol Allergy 6:3. https://doi.org/10.1186/1476-7961-6-3

10. Rana S (2018) Incense sticks: a potential source of indoor air pollution. Int J Environ Eng Manag 9:1–6

11. Lowden LA, Hull TR (2013) Flammability behaviour of wood and a review of its methods of reduction. Fire Sci Rev 2:4. https://doi.org/10.1186/2193-0414-2-4

12. Ovington JD, Madgwick HAI (1958) The sodium, potassium, and phosphorous contents of three species grown in close stands. New Phytol 57:273–284

13. Narayan N, Ashwathanarayan B (2022) Personal communication

14. Raman CV, Nedungadi TMK (1940) The alpha–beta transformation of quartz. Nature 145:147

15. Weber JN, Greer RT (1965) Dehydration of serpentine: heat of reaction and reaction kinetics. Am Miner 50:450–464

16. Momah M, Okieimen FE (2020) Minerology, geochemical composition and geotechnical properties of termite mound soil. J Ecol Nat Environ 12:1–8

17. Hrsak D, Sucik G, Lazic L (2008) The thermophysical properties of serpentinite. Metalurgija 47:29–31

18. Zulumyan N, Isahakyan A, Beglaryan H et al (2018) A study of thermal decomposition of antigorite from dunite and lizardite from peridotite. J Therm Anal Calorim 131:1201–1211. https://doi.org/10.1007/s10973-017-6705-6

19. Ferrand TP (2019) Neither antigorite nor its dehydration is "metastable". Am Minerol 104:88–790

20. Perrillat JP, Daniel I, Koga KT, Reynard B, Cardon H, Crichton WA (2005) Kinetics of antigorite dehydration: a real-time X-ray diffraction study. Earth Planet Sci Lett 236:899–913

21. Putz H, Brandenburg K (2022) Match! phase analysis using powder diffraction, version 3.x, crystal impact. https://www.crystalimpact.de/match

22. Gualtieri AF, Giacobbe C, Viti C (2012) The dihydroxylation of serpentine group minerals. Am Minerol 97:666–680

23. Chollet M, Daniel I, Koga KT, Morarad G, van Moortele B (2011) Kinetics and mechanism of antigorite dehydration: implication for subduction seismicity. J Geophys Res 116:B04203. https://doi.org/10.1029/2010JB007739

24. Gurtekin G, Albayrak M (2006) Thermal reaction of antigorite: a XRD, DTA-TG work. Miner Res Exp Bull 133:41–49